Revealing the hidden hyperfine interactions in ϵ-iron

Dimitrios Bessas,[1,*] Ilya Sergueev,[2] Konstantin Glazyrin,[2] Cornelius Strohm,[2] Ilya Kupenko,[1,†] Daniel G. Merkel,[1,‡] Gary J. Long,[3] Fernande Grandjean,[3] Aleksandr I. Chumakov,[1] and Rudolf Rüffer[1]

[1]*ESRF - The European Synchrotron, F-38043 Grenoble, France*

[2]*Deutsches Elektronen-Synchrotron, D-22607 Hamburg, Germany*

[3]*Department of Chemistry, Missouri University of Science and Technology, University of Missouri, Rolla, Missouri 65409-0010, USA*

(Received 15 March 2019; published 8 January 2020)

Herein, evidence for the long-sought finite hyperfine interaction in the high-pressure hexagonal close-packed ϵ-iron is gained through synchrotron radiation perturbed angular correlation spectroscopy. This method yields an energy splitting of 3.5(5) neV between the $m_{I_e} = \pm 1/2$ and $m_{I_e} = \pm 3/2$ nuclear sublevels of the iron-57 14.412-keV nuclear excited state at 30(1) GPa and room temperature. This energy splitting is related to a nuclear quadrupole hyperfine interaction with an electric field gradient of $eq = 1.2(2) \times 10^{16}\,\mathrm{V/cm^2}$. However, there is still a possibility that the splitting of the iron-57 nuclear levels is related to a modest magnetic hyperfine interaction of ca. 0.40(5) T.

DOI: 10.1103/PhysRevB.101.035112

I. INTRODUCTION

Iron is by mass the most abundant element on Earth [1] and, for several thousand years, its important properties have been exploited in diverse applications, ranging from direction finding, to biology, to structural materials. The pressure-temperature phase diagram of iron indicates that a martensiticlike transition from the familiar ambient pressure and temperature, ferromagnetic body-centered-cubic α-iron phase to a nonmagnetic hexagonal-closed-packed ϵ-iron, also known as hexaferrum, takes place in the pressure-temperature phase space with pressures above ca. 11 GPa and temperatures below ca. 1100 K and seems to coincide with a loss of ferromagnetic long-range order [2–4]. The pure ϵ-iron phase, as expected for all nonmagnetic metals, exhibits below 2 K and pressures between 15 and 30 GPa a transition to a superconducting state [5]. Theoretical predictions suggest an unconventional nature for the superconductivity which possibly arises from spin fluctuations [6]. Moreover, superconductivity in ϵ-iron was shown to be remarkably sensitive to the presence of defects [7] that are expected to affect the local structure. Local spatial structural fluctuations on the microscale caused by structural defects and stresses may also play a major role in the martensitic transformation of α-iron to ϵ-iron [8,9].

The ϵ-iron phase is expected to be the dominant [2–4] phase in the inner core of the Earth [10] and a unitless magnetic susceptibility as small as 10^{-3} is thought to be sufficient to stabilize the geodynamo, i.e., a proposed mechanism for generating the magnetic field of the Earth [11]. The observation of a magnetic hyperfine interaction in ϵ-iron may help to better understand the origin of this magnetic field. Thus, the contribution of an arguably small, perhaps a yet to be discovered, hyperfine magnetic and/or quadrupolar interaction in ϵ-iron, may improve the scientific understanding in disciplines ranging from solid state physics to geoscience. As a result, the distortion in the local crystal and electronic structure and the potential remnant magnetism in ϵ-iron have been extensively investigated using a wide range of techniques (see, e.g., Refs. [2,12–16]).

The local electronic structure as well as the static and dynamic magnetic order in a material may be probed through the measurements of hyperfine interactions by various well-established techniques. In some nickel-iron alloys no magnetic internal hyperfine field has been detected [17]. In contrast, the presence of hyperfine interactions has been proposed in ϵ-iron and other related hexagonal-closed-packed compounds. A sizable electric field gradient has been reported in some hexagonal closed-packed alloys [18] of iron with the isoelectronic valence d electrons ruthenium and osmium, as well as in both metallic cobalt [19] and metallic osmium [20]. The extrapolation of the antiferromagnetic transition temperature of the hexagonal-close-packed alloys of iron with ruthenium and osmium suggests [18] that ϵ-iron should exhibit a Néel temperature of ca. 100 K and a magnetic hyperfine field of ca. 1.6 T. A broadening of the iron-57 Mössbauer spectral resonance line in ϵ-iron as a function of pressure has been reported by Williamson *et al.* [12] and attributed to a quadrupolar electric hyperfine interaction leading to a quadrupole splitting of 0.17(3) mm/s. However, the origin and the presence of such a broadening has been highly debated [13,14].

The commonly used techniques for the measurements of hyperfine interactions are conventional Mössbauer spectroscopy, the nuclear forward scattering (NFS) of synchrotron radiation, and nuclear magnetic resonance spectroscopy. Unfortunately, none of these techniques provides an

*bessas@esrf.fr

†Present address: Institut für Mineralogie, Universität Münster, D-48149 Münster, Germany.

‡Permanent address: Institute for Particle and Nuclear Physics, Wigner Research Centre for Physics, Hungarian Academy of Sciences, H-1525 Budapest, Hungary.

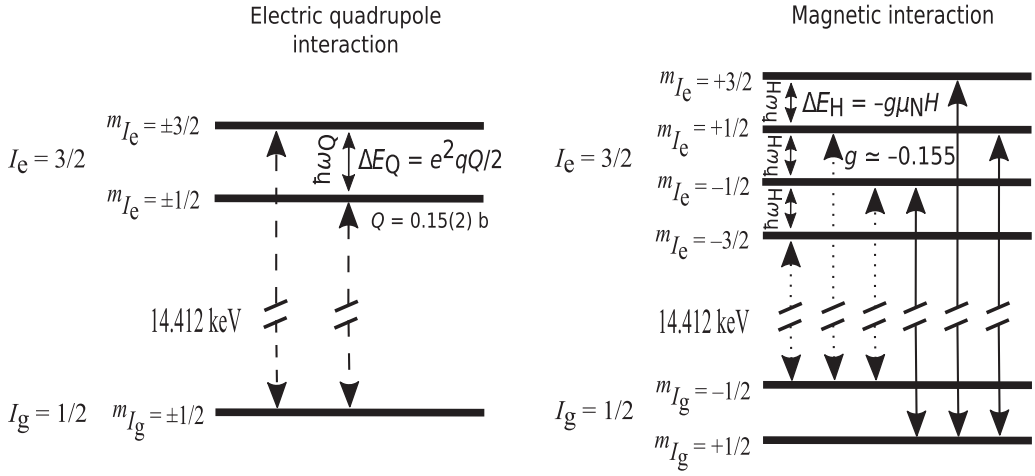

FIG. 1. Nuclear energy level diagrams for the 14.412-keV magnetic dipole (M1), nuclear transition in iron-57 (left) for a pure electric quadrupole interaction, and (right) for a pure magnetic hyperfine field interaction. Angular momentum I and angular-momentum projections m_I are shown close to the energy levels of the ground g and the excited e state. Transition lines relevant to a single ground state are indicated by different line types. The energy splitting $\Delta E_Q = \hbar\omega_Q$ and $\Delta E_H = \hbar\omega_H$ between the levels of the excited states for a pure electric quadrupole interaction and a pure magnetic hyperfine interaction, respectively, are shown.

unambiguous interpretation for the presence of hyperfine interactions in ϵ-iron. Indeed, nuclear magnetic resonance is insensitive to the electric field gradients because the nuclear quadrupole moment of the ground state in iron-57 is zero. Mössbauer spectroscopy is equally limited when the hyperfine interactions yield effects comparable to or smaller than the natural linewidth Γ_0 of the first nuclear excited state, which for iron-57 is 4.66 neV or 0.0970 mm/s. In the case of nuclear forward scattering of synchrotron radiation, it is difficult to distinguish between small hyperfine interactions and the small variations in the geometrical sample thickness.

Alternatively, time differential perturbed angular correlation spectroscopy is potentially a superior method [21,22] for identifying a small energy splitting between nuclear energy levels. This type of spectroscopy has two advantages over Mössbauer spectroscopy and NFS. The measured spectra are independent of both the sample thickness and the broadening in excess of the radioactive source natural linewidth [23]. Synchrotron radiation perturbed angular correlation spectroscopy [24] (SRPAC) combines the advantages of time differential perturbed angular correlation with the advantages of synchrotron radiation, i.e., high brilliance and focusing capabilities. These combined advantages make possible the study of subtle hyperfine interactions at extreme conditions.

The relatively unconventional technique of SRPAC has great potential and was indeed used to study the properties of Mössbauer active nuclei, e.g., iron-57 [24], tin-119 [25], nickel-61 [26]. SRPAC may be also used with less-known Mössbauer active nuclei [27] both in the solid or liquid phase. This technique probes isolated nuclei and is independent of recoil-free fraction [28,29]. The synchrotron radiation is used to incoherently excite the nuclei, i.e., the excited transitions originate from a single ground state and terminate in a metastable state that decays towards the ground state by different paths determined by the hyperfine interactions between the nuclei and their electronic environment (see Fig. 1). The experimental arrangement is shown in Fig. 2 and described in detail in Sec. II.

The reader should note that, although SRPAC and NFS are carried out using a very similar instrumentation, they are two essentially different experimental techniques. In short, NFS is an elastic coherent method that probes collective effects over a nuclear ensemble and thus is extremely sensitive to sample thickness, whereas SRPAC is an incoherent method and thus is in principle insensitive to sample thickness. Notably, NFS takes place by definition only in the forward direction, whereas SRPAC scattering occurs in the full solid angle. For more details on the differences between NFS and SRPAC, the reader should consult Ref. [30].

A preliminary SRPAC study [31] of α-iron, with an energy bandwidth of 15 meV, as expected, shows the presence of clear high-frequency modulations of the signal resulting from the magnetic hyperfine field present in α-iron [see Figs. 3(b)

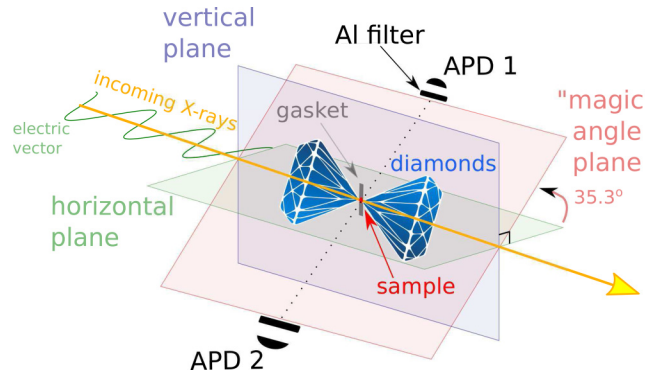

FIG. 2. The experimental arrangement used in this study includes an iron-57 enriched sample compressed in a diamond anvil cell and a set of detectors, APD1 and APD2, which are mounted together on a rotation stage with a rotation axis collinear with the incoming x-ray beam, and covered with aluminum filters (see text). The relative positions of the vertical scattering plane (blue), the horizontal scattering plane (green), a plane which coincides with the polarization plane of the incoming x-ray beam, and the third "magic" angle plane at 35.3° from the horizontal plane (red), are shown.

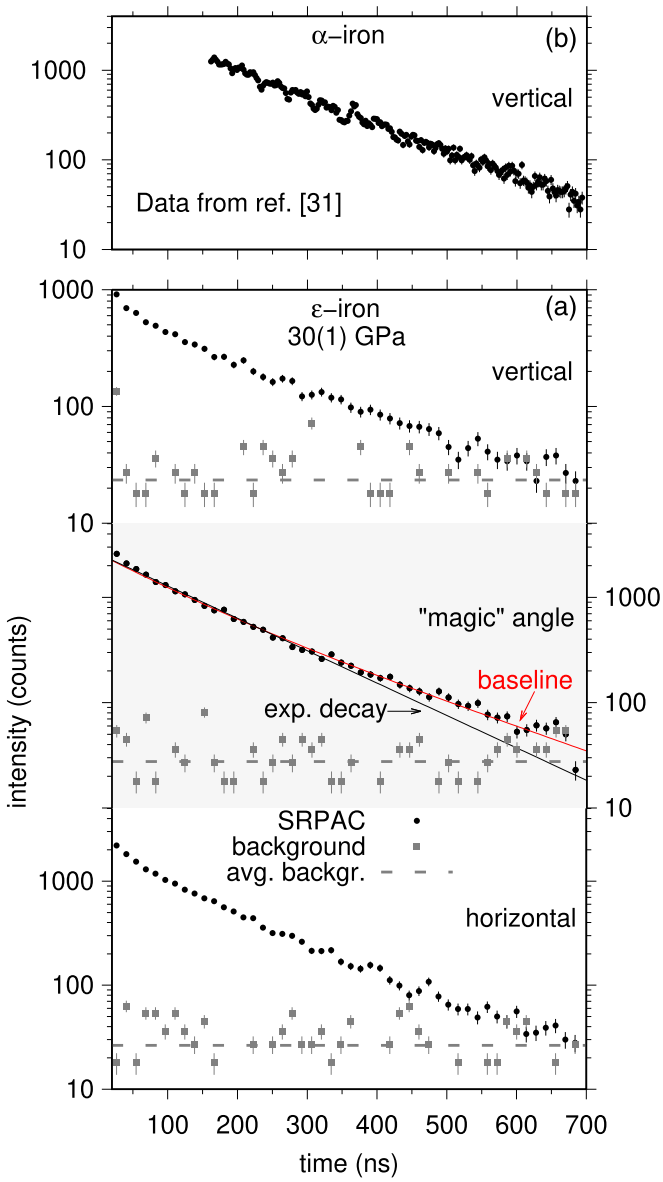

FIG. 3. (a) The time dependence of the incoherent scattering intensity, SRPAC, of ϵ-iron (black circles), in horizontal scattering geometry (lower plot), at the "magic" angle plane (center plot), and in vertical scattering geometry (top plot); the corresponding background measurements (gray squares) and the average background (dashed line) for each geometry measured at 30(1) GPa are shown. Typical uncertainties are given in each plot. An exponential decay with the lifetime of the first excited state of iron-57, 141.11 ns, (black line) and a fit of data measured at the "magic" angle with a baseline (red line) described in the text are also shown in the center plot. (b) The time dependence of the incoherent scattering intensity of α-iron (black symbols) in vertical scattering geometry is shown.

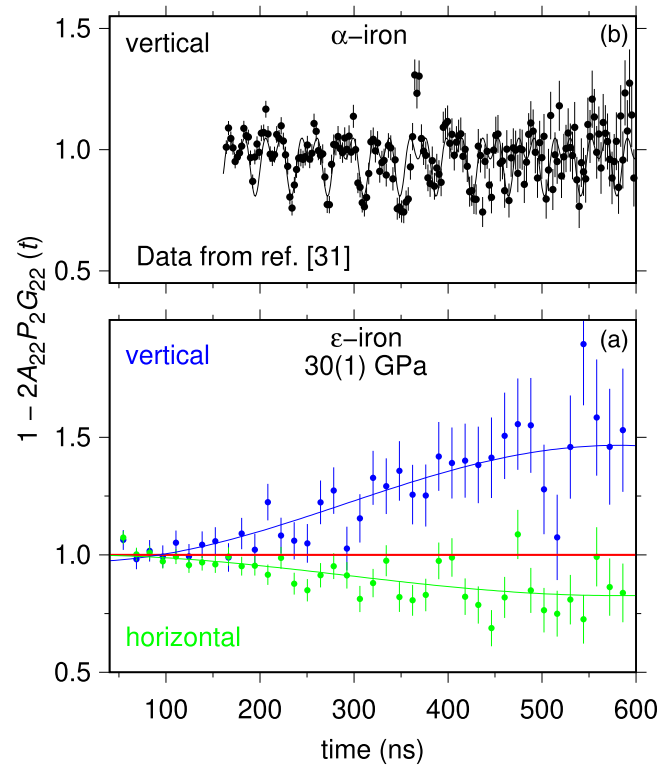

FIG. 4. The time dependence of the anisotropy factor in the SRPAC signal, $1 - 2A_{22}P_2G_{22}(t)$, (a) in ϵ-iron at 30(1) GPa in both the vertical (blue symbols) and horizontal (green symbols) scattering geometry, and (b) in α-iron in the vertical scattering geometry (black symbols). The horizontal red line in (a) is a visual guide for the absence of a hyperfine interaction. The blue and the green lines in (a) and the black line in (b) result from the fit carried out with the model described in Eq. (1) using a pure electric quadrupole interaction in (a) and a pure magnetic hyperfine interaction in (b).

and 4(b)]. The SRPAC study of the same iron sample at 13(1) and 25(1) GPa applied pressure revealed a lower-frequency modulation, however, the model involved in the data interpretation could not unambiguously determine an electric or a magnetic hyperfine interaction, because (i) the measurements were carried out in the pressure region where the martensitic transition takes place, thus, a remaining magnetic field from the low-pressure phase was still a possibility, and (ii) a dominant baseline was involved in the measurements because of complex multiple scattering effects related to the fact that the tails of the energy bandpass overlapped with the nuclear resonance energy.

Herein, in an attempt to solve these problems, we report a SRPAC study of ϵ-iron at 30(1) GPa and ambient temperature, with a narrower energy bandwidth of 2 meV. The spatial anisotropy of the SRPAC data in the presence of a hyperfine interaction, either electric or magnetic, is fully investigated through measurements in three different planes. We favor the presence of a finite electric quadrupole hyperfine interaction in ϵ-iron. However, the presence of a magnetic or combined electric and magnetic hyperfine interaction is still a possibility. Finally, our study demonstrates that SRPAC might be a method of choice for the systematic characterization of subtle electronic and spin state transitions inaccessible by the other methods mentioned above.

II. EXPERIMENTAL METHOD

The SRPAC measurements were carried out at the Nuclear Resonance beamline [32] ID18 at the European Synchrotron Radiation Facility.

We used a small piece of polycrystalline body-centered-cubic α-iron that had been 96% enriched in ^{57}Fe. The phase purity of the sample was confirmed by using x-ray diffraction at the PETRAIII beamline P02.2. The sample, with approximate lateral dimensions $20 \times 20\ \mu m^2$, was loaded, along with several ruby chips into a preindented beryllium gasket with an initial thickness of ca. 40 μm and a hole diameter of ca. 130 μm, between two diamond anvils with a 300-μm culet diameter. Paraffin was used as a pressure transmitting medium [33]. The pressure at the sample was measured before and after the actual SRPAC measurement by using the ruby fluorescence method. The x-ray beam was focused using two multilayer mirrors in the Kirkpatrick-Baez configuration to a spot with a 5 μm vertical height and a 13 μm horizontal width.

In this study, the time-resolved SRPAC data were measured at 30(1) GPa at the experimentally determined maximum on the phonon creation side in the nuclear inelastic scattering spectrum of ϵ-iron, i.e., +24 meV relative to the nuclear resonance energy. In addition, background measurements on the phonon annihilation side, i.e., −200 meV relative to the nuclear resonance energy, were carried out in sequence with the actual SRPAC measurements. Each SRPAC spectrum was measured for about 9 h. The time dependence of the SRPAC signal was detected between 20 and 700 ns after the arrival of the x-ray pulse, which in the four bunch synchrotron operating mode at ESRF, arrives every 704 ns, by using two avalanche photodiode detectors [34] (APDs), each with a 200-μm-thick active square area of 100 mm^2. The APDs were placed at a distance of ca. 6 mm from the sample on opposite sides of the pressure cell perpendicular to the diamond cell compression axis; see Fig. 2. Such a distance was experimentally found to be the best compromise between collected intensity and the angular resolution. The APDs were covered with a 320-μm-thick high-purity aluminum foil in order to reduce to ca. 0.02% the spatially isotropic and hyperfine interaction unmodulated delayed 6.4-keV iron $K\alpha$ fluorescence arising from nuclear internal conversion. A monochromator with a narrow energy bandwidth of 2 meV (full width at half maximum) at the nuclear resonance energy of iron-57 at 14.412 keV was employed to decrease the contribution of the Rayleigh scattering that follows the nuclear forward scattering events [29].

The SRPAC spectra have been measured in three geometries with the detectors perpendicular to the beam path (see Fig. 2). The scattering has been measured first in the vertical plane, second in the horizontal plane, i.e., the plane that is coincident with the polarization plane of the incoming x-ray beam, and third, in the so-called "magic" angle plane [35,36], that makes an angle of 35.3° with the horizontal plane, as shown in Fig. 2. Both the detectors and the diamond anvil cell were rotated together while changing the experimental geometry. This ensures keeping all geometrical parameters of the setup identical for all three geometries of scattering. Furthermore, for all geometries, the focused beam at the sample was kept on the same spot, within the $5 \times 13\ \mu m^2$ beam size.

III. RESULTS AND DISCUSSION

Figure 3(a) shows the time dependence of the SRPAC data and the measured background at 30(1) GPa in different geometries. This pressure was selected in order to ensure the full transformation of α-iron into the ϵ-iron phase. No periodic high-frequency modulations have been observed in the measured data; the absence of any of such modulations indicates the absence of high-field magnetic hyperfine interactions. The nuclear decay with the lifetime of the first excited state of iron-57 of $\tau = 141.11$ ns is shown as a straight black line in the middle portion of Fig. 3(a). A fit of the data measured at the "magic" angle with a baseline described below is shown as a red line.

The synchrotron radiation is highly linearly polarized with the electric vector lying in the horizontal plane. In the case of randomly oriented hyperfine fields all nuclear transitions coming from a single nuclear ground state will be excited (see Fig. 1). The time dependence of the SRPAC signal is given [26,29] by Eq. (1),

$$I(t) = I_0 \exp(-t/\tau)[1 - 2A_{22}P_2G_{22}(t)], \tag{1}$$

where I_0 is the intensity scaling factor, A_{22} is the anisotropy factor, which is determined by both the nuclear transition and details of the experimental arrangement, P_2 is a scattering geometry factor, i.e., $P_2 = 1$ for the vertical geometry, $P_2 = -1/2$ for the horizontal geometry, and $P_2 = 0$ for the magic angle geometry, $G_{22}(t)$ is the perturbation factor, which describes the time modulation of the signal due to hyperfine interactions, i.e., $G_{22}^{\mathrm{mag}}(t) = (1/5)(1 + 2\cos\omega_{\mathrm{H}}t + 2\cos 2\omega_{\mathrm{H}}t)$ for a magnetic hyperfine interaction, and $G_{22}^{\mathrm{el}}(t) = (1/5)(1 + 4\cos\omega_{\mathrm{Q}}t)$ for an electric hyperfine interaction, where $\omega_{\mathrm{H,Q}}$ is the characteristic angular frequency of the modulation [26,29].

For the data measured in the magic angle geometry, because P_2 is zero, the hyperfine interactions do not contribute to the signal and only a simple exponential nuclear decay should be observed [see Eq. (1)]. However, it is evident from Fig. 3(a) that the data at times longer than 400 ns depart from the exponential decay characteristic of the iron-57 nuclear excited state, as shown by the black straight line in Fig. 3(a). This observed departure cannot be related to the background, the magnitude of which is comparable with the actual data only for times longer than 600 ns. The origin of this departure is complex and is best described as a combination of two factors, such as potential radiation trapping effects [37] and/or nontrivial multiple scattering phenomena [38], factors that are independent of the scattering geometry. Thus, measurements in the magic angle geometry have been used in order to consistently eliminate such effects from the vertical and the horizontal scattering signals. The impact of these phenomena have been quantified in our analysis by replacing $\exp(-t/\tau)$ in Eq. (1) by $\exp(-t/\tau)[1 + a(t/\tau) + b(t/\tau)^2]$, where a and b are the only adjustable parameters. Thus, by fitting the data measured in the magic angle geometry, a well-defined baseline with $a = -6(1) \times 10^{-4}$ and $b = 2.7(3) \times 10^{-6}$ has been obtained and is shown as a red line in the central portion of Fig. 3(a).

Figure 4 shows the data for the vertical and the horizontal scattering geometries, divided by the baseline extracted from the data measured in the magic angle geometry. Low-frequency modulations with opposite sign in the horizontal and vertical geometry are clearly observed. These modulations reveal the presence of hyperfine interactions, as

described in Eq. (1). Both horizontal and vertical geometry data have been simultaneously fitted between 60 and 600 ns with the common fitting parameters A_{22} and ω, and a scaling factor I_0 for each geometry. The resulting fitted curves are shown in Fig. 4(a) as blue and green lines for the vertical and horizontal geometries, respectively. The modulation observed at 30(1) GPa in ϵ-iron [see Fig. 4(a)] has a period longer than 600 ns and can be fitted with either an electric or a magnetic hyperfine interaction.

By assuming a pure electric hyperfine interaction, the extracted angular frequency, $\omega_Q = 0.0054(7)$ rad/ns, corresponds to an energy splitting of $\Delta E_Q = 3.5(5)$ neV between the $m_{I_e} = \pm 1/2$ and $m_{I_e} = \pm 3/2$ sublevels of the iron-57 nuclear excited state; see Fig. 1. An electric field gradient, $eq = 1.2(2) \times 10^{16}\,\mathrm{V/cm^2}$, has been calculated from $\omega_Q = e^2qQ/2\hbar$, where e is the charge of the proton, $\hbar$ is the reduced Planck constant, and Q is the nuclear quadrupole moment of the iron-57 first excited state [39], 0.15(2) b. In the velocity scale of conventional Mössbauer spectroscopy, this electric field gradient eq would lead to a quadrupole splitting, $\Delta E_Q = 0.074(8)\,\mathrm{mm/s}$ or $0.76(8)\Gamma_0$.

By assuming a pure magnetic hyperfine interaction, a maximum value for the hyperfine magnetic field H has been calculated from the extracted angular frequency, $\omega_H = 0.0030(4)$ rad/ns, by using $\omega_H = -g\mu_N H/\hbar$, where $g \simeq -0.155$ is the g-factor of the iron-57 first nuclear excited state and $\mu_N = 5.050\,783\,53(11) \times 10^{-27}$ J/T is the nuclear magneton. Thus, a magnetic hyperfine field of 0.40(5) T and its associated energy splitting, between any pair $(m_{I_e}, m_{I_e} - 1)$ of levels of the $I_e = 3/2$ iron-57 nuclear excited state, $\Delta E_H = 2.0(3)$ neV, have been obtained (see Fig. 1). The magnitude of this magnetic hyperfine field is below the upper limit of 0.5 T at 5 K obtained from an externally applied magnetic field transmission Mössbauer spectral study [40]. The herein extracted hyperfine field of 0.40(5) T corresponds to a magnetic splitting between the external lines of a conventional Mössbauer spectral magnetic sextet of $\Delta E_H = 0.12(2)\,\mathrm{mm/s}$, or ca. $1.2(2)\Gamma_0$.

A hint as to the nature of the hyperfine interaction is given by the quality factor of the fit; the reduced χ^2 for the electric hyperfine interaction is 1.035, whereas the reduced χ^2 for the magnetic hyperfine interaction is 1.059. As a result, the analysis of the SRPAC data obtained in this study favors the presence of an electric quadrupole interaction in ϵ-iron at 30(1) GPa and room temperature. The preference of an electric quadrupole interaction over a hyperfine magnetic field is also in agreement with the analysis of the anisotropy factor A_{22} reported in Ref. [31]. Thus, although the electric or magnetic origin of the observed hyperfine interaction cannot be unquestionably derived, the experimental results and their analysis provide some support favoring the electric quadrupole hyperfine interaction as the origin of the observed hyperfine splitting.

For ϵ-iron as a function of applied pressure, Williamson *et al.* [12] measured a Mössbauer spectral linewidth of ca. 0.6 mm/s at ca. 15 GPa. The natural width, the instrumental linewidth broadening, the linewidth broadening due to the finite thickness of the sample, and the linewidth broadening from self-absorption in the source account for a minimum experimental linewidth of 0.41 mm/s in their experiment. The excess linewidth of 0.19 mm/s was analyzed as the sum of a contribution of 0.08(3) mm/s from a partial transformation of α-iron to ϵ-iron at 15 GPa and a contribution of 0.11(3) mm/s due to a hyperfine interaction. From the latter contribution to the broadening, Williamson *et al.* [12] have estimated a quadrupole splitting of 0.17(3) mm/s and thus a hyperfine splitting of 8.16 neV between the $m_{I_e} = \pm 3/2$ and $\pm 1/2$ sublevels of the $I_e = 3/2$ nuclear excited state of iron-57. The total splitting of 8.16 neV at ca. 15 GPa is about twice that of 3.5(5) neV measured herein at 30(1) GPa.

The quadrupole splitting is the sum of two contributions, first, the lattice contribution, and second, the anisotropy contribution because of the nonsphericity of the local conduction electron distribution. Williamson *et al.* [12], based on a point charge model [13], calculated a lattice contribution to the quadrupole splitting [41] for ϵ-iron of ca. 0.03 mm/s or an energy splitting of 1.5 neV, if $Q = 0.2$ b is used, or of ca. 0.02 mm/s and a splitting of 1.0 neV, if $Q = 0.15$ b is used, as stated herein. The c/a ratio in ϵ-iron between 15 and 30 GPa changes by less than 0.1% [42,43]. It is thus reasonable to assume that the same lattice contribution to the quadrupole splitting is involved in our study as in the study by Williamson *et al.* [12].

Consequently, depending upon whether the two components add or subtract from each other, an anisotropy contribution from the nonsphericity of the local conduction electron distribution to the quadrupole splitting of either 0.054(8) mm/s, i.e., a splitting of ca. 2.5(5) neV or 0.094(8) mm/s, i.e., a splitting of ca. 4.5(5) neV, has been obtained in this study at 30(1) GPa. In comparison, a contribution of 0.15 mm/s, i.e., a splitting of ca. 7.2 neV or a contribution of 0.19 mm/s, i.e., a splitting of ca. 9.2 neV has been obtained by Williamson *et al.* [12] at ca. 15 GPa.

Thus, the difference in the hyperfine splitting measured herein, 3.5(5) neV at 30(1) GPa, and that obtained by Williamson *et al.* [12], 8.16 neV at ca. 15 GPa, indicates either a significant reduction in the anisotropy contribution because of the nonsphericity of the local conduction electron distribution to the quadrupole splitting by more than a factor of 2 or an underestimation by Williamson *et al.* [12] in one of the components that broaden the Mössbauer spectral line.

The local environment is not only important for structural phase transitions but is equally important for transitions to the superconducting state. Structural defects have been reported [8,9] as the most reasonable driving force for the martensite to ϵ-iron transformation. The importance of structural defects has been investigated by Holmes *et al.* [7] who found that superconductivity in ϵ-iron is sensitive to structural defects and can be destroyed and recovered by mechanical work and annealing, respectively. In support of this relationship, our study reveals the presence of a measurable, nonzero, electric field gradient which could be intrinsically correlated with defects [44].

Alternatively, after considering several possible scenarios, Holmes *et al.* [7] suggested that strong interactions between electrons and spin fluctuations may also be responsible for superconductivity in ϵ-iron. Our study reveals the possible presence of a measurable, nonzero, magnetic hyperfine field at the iron-57 nucleus in ϵ-iron at room temperature and 30(1) GPa as a result of spin fluctuations similar to those

involved in nonmagnetic palladium [45]. Hence, the results reported herein are compatible with the two likely origins for superconductivity in ϵ-iron.

IV. CONCLUSION

We studied the hyperfine interactions in iron at room temperature and pressure of 30(1) GPa by synchrotron radiation perturbed angular correlation spectroscopy. We report the presence of a long-sought interaction between the electronic and the nuclear systems which leads to an energy splitting in the nuclear levels of iron-57. We demonstrate that synchrotron radiation perturbed angular correlation spectroscopy (SRPAC) is a straightforward way to identify subtle electronic or spin state transitions which are inaccessible with other techniques in compounds containing Mössbauer active isotopes.

Herein, for ϵ-iron at ambient temperature and 30(1) GPa applied pressure by assuming a pure electric quadrupole hyperfine interaction, SRPAC yields an energy splitting, $\Delta E_{\mathrm{Q}} = 3.5(5)$ neV, between the $m_{I_{\mathrm{e}}} = \pm 1/2$ and $m_{I_{\mathrm{e}}} = \pm 3/2$ nuclear sublevels of the iron-57 nuclear excited state. This energy splitting is related to an electric field gradient of $eq = 1.2(2) \times 10^{16}\,\mathrm{V/cm^2}$. Alternatively, by assuming a pure magnetic hyperfine interaction, an energy splitting, $\Delta E_{\mathrm{H}} = 2.0(3)$ neV, between any pair $(m_{I_{\mathrm{e}}}, m_{I_{\mathrm{e}}} - 1)$ of levels of the $I_{\mathrm{e}} = 3/2$ iron-57 nuclear excited state, is obtained and corresponds to a magnetic hyperfine field H of 0.40(5) T. The smaller value of χ^2 of the fit slightly favors the presence of an electric quadrupole interaction but does not exclude the presence of a magnetic hyperfine field interaction. A definitive answer about the nature of the hyperfine interaction present in ϵ-iron at ambient temperature and applied pressure equal to or greater than 30(1) GPa requires obtaining SRPAC data at times longer than 700 ns with a more brilliant x-ray source. These experimental conditions are unavailable at this time but might be available in the near future [46].

ACKNOWLEDGMENTS

The European Synchrotron Radiation Facility is acknowledged for beamtime provision at the Nuclear Resonance beamline ID18. We thank J.-P. Celse for technical assistance during the experiment and Prof. L. Dubrovinsky for providing the diamond anvil cell.

[1] J. W. Morgan and E. Anders, Proc. Natl. Acad. Sci. USA **77**, 6973 (1980).
[2] O. Mathon, F. Baudelet, J. P. Itié, A. Polian, M. d'Astuto, J. C. Chervin, and S. Pascarelli, Phys. Rev. Lett. **93**, 255503 (2004).
[3] M. Nicol and G. Jura, Science **141**, 1035 (1963).
[4] D. Bancroft, E. L. Peterson, and S. Minshall, J. Appl. Phys. **27**, 291 (1956).
[5] K. Shimizu, T. Kimura, S. Furomoto, K. Takeda, K. Kontani, Y. Onuki, and K. Amaya, Nature (London) **412**, 316 (2001).
[6] G. Steinle-Neumann, L. Stixrude, and R. E. Cohen, Proc. Natl. Acad. Sci. USA **101**, 33 (2004).
[7] A. T. Holmes, D. Jaccard, G. Behr, Y. Inada, and Y. Onuki, J. Phys.: Condens. Matter **16**, S1121 (2004).
[8] A. Dewaele, C. Denoual, S. Anzellini, F. Occelli, M. Mezouar, P. Cordier, S. Merkel, M. Véron, and E. Rausch, Phys. Rev. B **91**, 174105 (2015).
[9] B. Dupé, B. Amadon, Y.-P. Pellegrini, and C. Denoual, Phys. Rev. B **87**, 024103 (2013).
[10] J. Garai, J. Chen, and G. Telekes, Am. Mineral. **96**, 828 (2011).
[11] S. Gilder and J. Glen, Science **279**, 72 (1998).
[12] D. L. Williamson, S. Bukshpan, and R. Ingalls, Phys. Rev. B **6**, 4194 (1972).
[13] R. D. Taylor, G. Cort, and J. O. Willis, J. Appl. Phys **53**, 8199 (1982).
[14] G. Cort, R. D. Taylor, and J. O. Willis, J. Appl. Phys **53**, 2064 (1982).
[15] J. P. Rueff, M. Krisch, Y. Q. Cai, A. Kaprolat, M. Hanfland, M. Lorenzen, C. Masciovecchio, R. Verbeni, and F. Sette, Phys. Rev. B **60**, 14510 (1999).
[16] A. Monza, A. Meffre, F. Baudelet, J.-P. Rueff, M. d'Astuto, P. Munsch, S. Huotari, S. Lachaize, B. Chaudret, and A. Shukla, Phys. Rev. Lett. **106**, 247201 (2011).
[17] A. B. Papandrew, M. S. Lucas, R. Stevens, I. Halevy, B. Fultz, M. Y. Hu, P. Chow, R. E. Cohen, and M. Somayazulu, Phys. Rev. Lett. **97**, 087202 (2006).
[18] H. Ohno, J. Phys. Soc. Jpn. **31**, 92 (1971).
[19] G. J. Perlow, C. E. Johnson, and W. Marshall, Phys. Rev. **140**, A875 (1965).
[20] D. Bessas, I. Sergueev, D. G. Merkel, A. I. Chumakov, R. Rüffer, A. Jafari, S. Kishimoto, J. A. Wolny, V. Schünemann, R. J. Needham *et al.*, Phys. Rev. B **91**, 224102 (2015).
[21] J. C. Soares, K. Krien, A. G. Bibiloni, K. Freitag, and R. Vianden, Phys. Lett. A **45**, 465 (1973).
[22] C. Hohenemser, R. Erno, H. Benski, and J. Lehr, Phys. Rev. **184**, 298 (1969).
[23] G. S. Collins and N. Benczer-Koller, Phys. Rev. B **17**, 2085 (1978).
[24] A. Q. R. Baron, A. I. Chumakov, R. Rüffer, H. Grünsteudel, H. F. Grünsteudel, and O. Leupold, Europhys. Lett. **34**, 331 (1996).
[25] C. Strohm, I. Sergueev, and U. van Bürck, Europhys. Lett. **81**, 52001 (2008).
[26] I. Sergueev, O. Leupold, H.-C. Wille, T. Roth, A. I. Chumakov, and R. Rüffer, Phys. Rev. B **78**, 214436 (2008).
[27] G. M. Kalvius, F. E. Wagner, and W. Potzel, J. Phys. Colloq. **37**, C6-657 (1976).
[28] M. A. Chuev, J. Exp. Theor. Phys. **103**, 243 (2006).
[29] I. Sergueev, U. van Bürck, A. I. Chumakov, T. Asthalter, G. V. Smirnov, H. Franz, R. Rüffer, and W. Petry, Phys. Rev. B **73**, 024203 (2006).
[30] I. Sergueev, Nuclear resonant scattering for the study of dynamics of viscous liquids and glasses, Ph.D. thesis,Technischen Univerität München, 2004.
[31] D. Bessas, I. Sergueev, K. Glazyrin, C. Strohm, I. Kupenko, D. G. Merkel, A. I. Chumakov, and R. Rüffer, Hyperfine Interact. **241**, 10 (2019).
[32] R. Rüffer and A. I. Chumakov, Hyperfine Interact. **97**, 589 (1996).
[33] Paraffin is known not to provide the best hydrostatic conditions at ca. 30 GPa. However, SRPAC is insensitive to isomer shifts

which might be related to potential pressure gradients in the pressure chamber. Thus, the recorded signal cannot be attributed to potential pressure gradients within the pressure chamber.

[34] A. Q. R. Baron, Hyperfine Interact. **125**, 29 (2000).

[35] The "magic" angle in this study is defined similarly to NMR (see Ref. [36]). Note that the complementary angle, i.e., 54.7°, may also be given in some studies.

[36] J. W. Hennel and J. Klinowski, *Magic-Angle Spinning: A Historical Perspective* (Springer, Berlin, 2005), pp. 1–14.

[37] A. I. Chumakov, J. Metge, A. Q. R. Baron, R. Rüffer, Yu. V. Shvyd'ko, H. Grünsteudel, and H. F. Grünsteudel, Phys. Rev. B **56**, R8455 (1997).

[38] F. J. Lynch, R. E. Holland, and M. Hamermesh, Phys. Rev. **120**, 513 (1960).

[39] G. Martínez-Pinedo, P. Schwerdtfeger, E. Caurier, K. Langanke, W. Nazarewicz, and T. Söhnel, Phys. Rev. Lett. **87**, 062701 (2001).

[40] S. Nasu, T. Sasaki, T. Kawakami, T. Tsutsui, and S. Endo, J. Phys.: Condens. Matter **14**, 11167 (2002).

[41] T. P. Das and M. Pomerantz, Phys. Rev. **123**, 2070 (1961).

[42] A. Dewaele, P. Loubeyre, F. Occelli, M. Mezouar, P. I. Dorogokupets, and M. Torrent, Phys. Rev. Lett. **97**, 215504 (2006).

[43] K. Glazyrin, L. V. Pourovskii, L. Dubrovinsky, O. Narygina, C. McCammon, B. Hewener, V. Schünemann, J. Wolny, K. Muffler, A. I. Chumakov *et al.*, Phys. Rev. Lett. **110**, 117206 (2013).

[44] R. Dogra, A. P. Byrne, and M. C. Ridgway, J. Electron. Mater. **38**, 623 (2009).

[45] S. Doniach, Proc. Phys. Soc., London **91**, 86 (1967).

[46] B. Adams, G. Aeppli, T. Allison, A. Q. R. Baron, P. Bucksbaum, A. I. Chumakov, C. Corder, S. P. Cramer, S. DeBeer, Y. Ding *et al.*, arXiv:1903.09317.